

Skin Lesion Segmentation: U-Nets versus Clustering

Bill S. Lin¹, Kevin Michael², Shivam Kalra³, H.R. Tizhoosh³

¹ Department of Mechanical and Mechatronics, University of Waterloo, Waterloo, Canada

² Department of Systems Design Engineering, University of Waterloo, Waterloo, Canada

³ KIMIA Lab, University of Waterloo, Waterloo, Canada

Abstract—Many automatic skin lesion diagnosis systems use segmentation as a preprocessing step to diagnose skin conditions because skin lesion shape, border irregularity, and size can influence the likelihood of malignancy. This paper presents, examines and compares two different approaches to skin lesion segmentation. The first approach uses U-Nets and introduces a histogram equalization based preprocessing step. The second approach is a C-Means clustering based approach that is much simpler to implement and faster to execute. The Jaccard Index between the algorithm output and hand segmented images by dermatologists is used to evaluate the proposed algorithms. While many recently proposed deep neural networks to segment skin lesions require a significant amount of computational power for training (i.e., computer with GPUs), the main objective of this paper is to present methods that can be used with only a CPU. This severely limits, for example, the number of training instances that can be presented to the U-Net. Comparing the two proposed algorithms, U-Nets achieved a significantly higher Jaccard Index compared to the clustering approach. Moreover, using the histogram equalization for preprocessing step significantly improved the U-Net segmentation results.

Keywords—Skin lesion Segmentation; U-Nets; C-Means Clustering; Melanoma; Histogram Equalization; Color Space

I. INTRODUCTION

With between 2 and 3 million cases occurring globally each year, skin cancer is the most common cancer worldwide [1], [2]. Since skin cancer occurs at the surface of the skin, melanomas, one of the world's most deadly cancer, can be diagnosed with visual inspection by a dermatologist [1], [3]. To improve the accuracy, dermatologists use a dermatoscope, which eliminates some of the surface reflection and enhances the deeper layers of skin [4]. Dermatologists often look for five specific signs when classifying melanomas. These include skin lesion asymmetry, irregular borders, uneven distribution of color, diameter, and evolution of moles over time [5]. Standard skin cancer computer-aided diagnosis systems include five important steps: acquisition, preprocessing, segmentation, feature extraction, and finally, classification [6]. Since the shape and border of the skin lesion is extremely important in the diagnosis, automatic diagnosis systems must be able to accurately identify and segment the skin lesion in the image.

Automatic skin lesion segmentation contains many different challenges. The lesion color, texture, and size can all vary considerably for different patients. On top of this, medical gauzes, hair, veins, and light reflections in the image make it even more difficult to identify the skin lesion. Finally, in the areas surrounding a skin lesion, there are often sub-regions that are darker than others. This makes it difficult to consistently identify which sub-regions are part of the lesion and which

sub-regions are just part of the surrounding skin. Finally, lack of large labeled datasets (segmented by dermatologists) makes training sophisticated networks rather difficult.

This paper presents and compares multiple approaches to automatic segmentation of dermoscopic skin lesion images. Firstly, we present some different segmentation approaches using U-nets including one with a novel histogram-based preprocessing technique. After this, the U-net approach is compared with a much simpler clustering algorithm. While U-nets and other deep networks often require a lot of training and computational power, the approaches presented in this paper are designed such that they do not require GPU power. All training and testing in this paper have been done with a single CPU.

The paper is organized as follows: Section II briefly reviews the literature of existing techniques for skin lesion segmentation. Section III describes the proposed dataset used to benchmark proposed methods. Section IV explains the proposed methods; results and conclusion are discussed in Section V and Section VI, respectively.

II. BACKGROUND REVIEW

Machine learning schemes like reinforcement learning and neural networks have been used for segmentation of medical images [19], [20], [21], [22], [23]. Since skin lesion segmentation is frequently used as an important first step in many automated skin lesion recognition systems, there have been many different approaches. A summary of several skin lesion segmentation methods by Celebi et al. [7] reviews many recent techniques proposed in literature. Frequently, proposed lesion segmentation techniques include a preprocessing step which removes unwanted artifacts such as hair or light reflections. Another very common preprocessing step involves performing color space transformation in order to make segmentation easier. Common techniques that have recently been proposed in the literature include, among others, histogram thresholding, clustering and active contours. Most recently, deep neural networks have led to many breakthroughs, producing excellent results in image segmentation [8].

Color space transformations can help facilitate skin lesion detection. For instance, Garnavi et al. [9], take advantage of RGB, HSV, HSI, CIE-XYZ, CIE-LAB, and YCbCr color spaces and use a thresholding approach to separate the lesion from the background skin. Similarly, Yuan et al. [10] use RGB, HSV, and CIE-LAB color spaces as input channels to a fully convolutional-deconvolutional neural network in order to segment the images.

Hair removal is a very common preprocessing step used to facilitate skin lesion segmentation. The presence of dark hairs on the skin often significantly degrades the performance of most automatic segmentation algorithms. For example, one very popular software, Dullrazor [11], identifies the dark hair locations using morphological operations. Afterwards, the hair pixels are replaced with nearby skin pixels and the resulting image is smoothed in order to remove the hair artifacts. Many recent techniques use similar morphology or diffusion methods to remove hair [6], [9], [12].

Once the image has been preprocessed, many different methods have been proposed for segmentation. Since most skin lesions are darker than the surrounding skin, thresholding is a very commonly used technique. However, further image enhancement algorithms need to be performed in order to make thresholding effective. For example, Fan et al. [6] propose first enhancing the skin lesion image using color and brightness saliency maps before applying a modified Otsu threshold method. Similarly, Garnavi et al. [9] use a thresholding based approach on 25 color channels from a variety of different color spaces in order to segment the images. Often with histogram thresholding, a connected components analysis needs to be performed after thresholding in order to remove medical gauzes, pen marks, or other artifacts that have been wrongly classified by thresholding.

Clustering-based methods are commonly used as well. For instance, Schmid-Saugeon et al. [12] propose using a modified Fuzzy C-Means clustering algorithm on the two largest principle components of the image in the LUV color space. The number of clusters for the Fuzzy C-Mean algorithm is determined by examining the histogram computed using the two principal components of the image. Melli et al. [13] propose using mean shift clustering to get a set of redundant classes which are then merged into skin and lesion regions.

More recently, convolutional neural networks and other deep artificial neural networks are proposed. Commonly, the image is first preprocessed to remove artifacts. Afterwards, a neural network is used to identify the lesion. For instance, in a work proposed by Jafari et al. [14], the image is first preprocessed using a guided filter before a CNN uses both local and global information to output a label for each pixel.

III. IMAGE DATA

The 2017 IEEE International Symposium on Biomedical Imaging (ISBI) organized a skin lesion analysis challenge for melanoma detection, ISIC 2017 (International Skin Imaging Collaboration). The challenge released a public set of 2000 skin lesion images that have been segmented and classified by dermatologists. There is also a validation and a test set that is not publicly available for the competition. Lesion segmentation is one of three parts of the competition. For evaluation, the Jaccard Index is used to rank the algorithms. This year, the vast majority of the participants, including the top submissions, used a deep neural networks to segment the images. For example, Yuan et al. [10] augmented the 2000 images using rotation, flipping, rotating, and scaling



Fig. 1. Sample skin lesion images from public data set used for ISBI 2017 challenge.

and trained a convolutional-deconvolutional neural network with 500 epochs. Clustering was also used in some submissions, although the performance of clustering algorithms were generally worse compared with that of the deep artificial networks. A variety of different evaluation metrics have been used in the literature. This includes the XOR measure, and Specificity, Sensitivity, Precision, Recall, and error probability [7]. The ISBI 2017 challenge used the Jaccard Index in order to evaluate methods. In order to compare the algorithms and methods proposed in this paper, the average Jaccard Index is used to evaluate the proposed method's performance.

The ISIC 2017 training set was used to both train and validate our approaches. This publicly available dataset contains a total of 2000 images including 374 melanoma, 254 seborrheic keratosis and 1372 benign nevi skin lesion images in JPG format. The images are in many different dimensions and resolutions. Each skin lesion has also been segmented by a dermatologist; the 2000 binary masks corresponding to each skin lesion image is provided in PNG format.

Figure 1 shows a collection of sample images from the data set. As can be seen from the images, there are many unwanted artifacts including reflections, hair, black borders, pen marks, dermatoscope gel bubbles, medical gauzes, and other instrument markings that make segmentation difficult. Furthermore, there is a high variability in skin lesion shape, size, color and location.

IV. METHODOLOGY

The main objective of this paper is to develop different approaches that can process skin lesion images, and produce a binary mask with 1 corresponding to pixels that are part of

the skin lesion, and 0 corresponding to pixels that are not part of the skin lesion. The output format should be identical to the binary masks segmented by the dermatologists in order to evaluate the performance of the segmentation algorithms.

In order to compare the performance of algorithms with that of other submissions in the ISBI challenge, the Jaccard Index, which was the challenge evaluation metric, is used. Since all of the approaches in this paper are performed without a GPU, some approaches, in particular, the ones involving a U-Net, take around several hours (in our case 8 hours) to train for each validation fold. In order for the validation to complete within a reasonable amount of time, 5 random cross validation folds were performed with a 90% training (1800 images) and 10% validation (200 images) split. In this methodology section, we first discuss the performance of U-Nets followed by clustering.

A. U-Net Approach

The U-Net architecture used in image segmentation uses a Python library for U-Nets by Akeret et al. [15] with the open source library TensorFlow. The architecture is based on the network proposed by Ronneberger et al. [16] for biomedical image segmentation (Figure 2). As discussed in the paper by Ronneberger et al., this network architecture can be trained with very few images and is relatively fast to train and test.

Because the goal of this paper is to develop an algorithm that works without the need of a GPU, the number of training iterations that can be done on the U-Net is severely limited. Unlike the top ISBI submissions that used Neural Networks, which augment the data to tens of thousands of images and set the number of epochs to a few hundred [10], the proposed network was trained with a lot less training iterations.

The 1800 images are first augmented to 7200 images by a combination of flips and rotations. Afterwards, just over one epoch (10,000 training iterations) is applied to train the network. This is roughly 1% of the number of training iterations used by the top submissions in the ISBI challenge.

1) *Architecture and Training:* Similar to convolutional neural networks, which repeatedly apply convolutions, activation functions and downsampling, the U-Net architecture extends this by including symmetric expansive layers which contain upsampling operators. The proposed architecture contains 4 contracting steps and 4 expansion steps. Each contraction step contains two unpadded 3×3 convolutions each followed by a ReLU activation function. Finally, a 2×2 max pooling operation is used for down sampling. In each down sampling step, the number of feature channels doubles.

In each expansion step, two unpadded 3×3 convolutions each followed by a ReLU activation function is used. However, instead of the 2×2 max pooling, an up-convolution layer is added which halves the number of feature channels. The features from the corresponding contraction layer are also concatenated in the expansion layer.

At the end, a final layer of a 1×1 convolution is used to map the feature vector to a desired binary decision. A pixel-wise soft-max is applied in order to determine the degree of which a certain pixel belongs to the skin lesion.

The loss function used is the cross entropy between the prediction and the ground truth. The Adam optimizer with a constant learning rate of 0.0002 is used to train the network. A dropout rate of 0.5 is used.

2) *Pre- and Post-Processing:* Before the data is sent to the U-Net, a few pre-processing steps are performed. Firstly, in order to increase the amount of contrast in the image, the image is converted to HSI color space, and histogram equalization is applied to the intensity (I) channel. After this, the image is converted back to RGB format. The reason for this equalization is that the contrast between the skin lesions (usually darker) is more noticeable compared to the surrounding skin (usually brighter). On top of this, as a 4th channel, the original intensity (I) channel with values normalized to between 0 and 1 is added. Finally, as a 5th channel, a 2-dimensional Gaussian centered at the middle of the image is generated. The full-width half maximum of the 2D Gaussian was set to be 125 pixels, which was roughly where most of the skin lesions lie within the center from a visual inspection of the training data.

To the authors' best knowledge, this is the first time that histogram equalization and an extra Gaussian channel is used as an input to a U-Net. The image needs to be rescaled and zero-padded so that the U-Net can perform segmentation. Each image is rescaled such that the largest dimension is 250 pixels. The smaller dimension is filled with white padding so that the image becomes 250×250 . Finally, in order to account for cropping due to the unpadded convolutions, the image is white padded with a border of 46 pixels so that the final size is 342×342 pixels.

After training, some post-processing steps are applied to the testing set in order to improve the result. Firstly, a morphology operation (using the "scipy" *binary_fill_holes* function) is applied to the image in order to fill the holes in the segmented image. After this, in order to find the best threshold to set for the U-Net output, a gradient descent is applied to the threshold using in order to determine the best threshold.

3) *U-Net Algorithm:* In order to test the effect of the pre-processing and post-processing, two different approaches are compared. One with the pre-/post-processing and one without pre-/post-processing. The exact same U-Net architecture, which is described in an earlier section, is used for both cases.

The pseudo-code in Figure 3 shows the algorithm without pre-/post-processing. The pseudo-code in Figure 4 shows the algorithm with pre/post-processing. The results obtained from the two approaches are discussed in a later section.

B. Clustering Algorithm

This approach leverages an unsupervised clustering technique to analyze the image and segment the lesion of interest. It uses Fuzzy C-means clustering in order to split the image up into a number of distinct regions of interest. It then leverages k-means clustering to group the clusters based on color features. Ultimately it selects the group of clusters with the darkest color features and identifies it to be the mole.

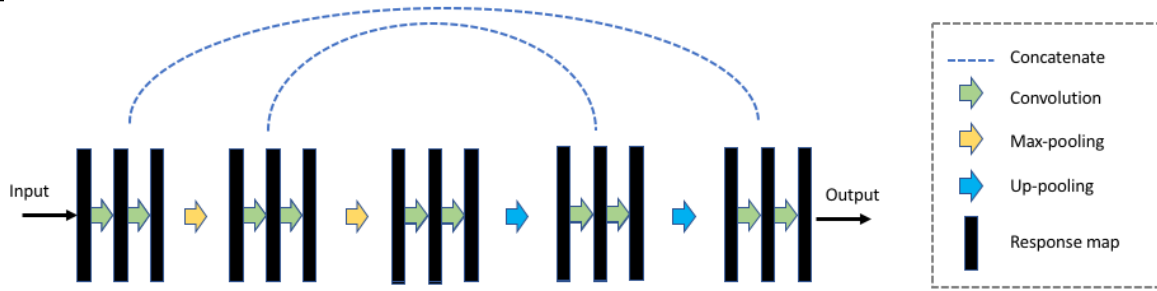


Fig. 2. Schematic illustration of U-Net according to [16].

U-Net Approach without Pre/Post-Processing (Algorithm 1A):

- 1) For each of 1800 Training RGB images:
 - a) Rescale RGB image such that largest dimension is 250 pixels
 - b) Normalize image to values between 0 and 1
 - c) White-Pad RGB image to 342x342 pixels
 - d) Add image to training set
- 2) Train U-Net with 10,000 iterations selected from the 1800 training images (This corresponds to just over 5 epochs)
- 3) Predict test data set using threshold of 0.5 and obtain Jaccard Index

Fig. 3. U-Net Algorithm without Pre-/Post-Processing (Algorithm 1A)

1) *Pre-Processing:* When conducting clustering to the images, there are two major sources of disturbance within the image. Firstly, the presence of hair on-top of the skin causes discrepancies in the algorithms ability to cluster, therefore strands of hair were removed in a pre-processing step which utilizes a morphological top-hat and thresholding technique. This technique is outlined in pseudo code in Figure 5.

Secondly, a subset of the images were captured using imaging devices with a circular field of view. Resultant images captured using this type of device were circular in nature with black pixels filling the outer boundaries of the circle. These pixels were removed from the area of analysis and the algorithm for doing so can be seen in Figure 6.

2) *Clustering Algorithm Summary:* The algorithm outlined in the above sections can be found summarized in the pseudo-code in Figure 7 and includes the pre-processing steps of hair removal and outer-circle removal. This algorithm will be referenced as Algorithm 2 for future sections. Experimentally, when $C = 5$, at least one of the clusters is the mole itself. For this reason, $C = 5$ was used for the algorithm.

U-Net Approach with Pre/Post-Processing (Algorithm 1B):

- 1) For each of 1800 Training RGB images:
 - a) Rescale RGB image such that largest dimension is 250 pixels
 - b) $Im_hsi = \text{Convert RGB image to HSI image}$
 - c) $I_orig = I \text{ channel of } Im_hsi$
 - d) Normalize I_orig to values between 0 and 1
 - e) Apply histogram equalization to I channel of im_hsi
 - f) $Train_img[\text{channels } 0, 1, 2] = \text{Convert } im_hsi \text{ to RGB}$
 - g) $Train_img[\text{channel } 3] = I_orig$
 - h) $Train_img[\text{channel } 4] = 2D \text{ Gaussian with } 125 \text{ pixel Full Width Half Maximum}$
 - i) Horizontally Flip, Vertically Flip, Rotate 180 $Train_img$ (This augments 1800 images to 7200)
 - j) White-Pad $Train_img$ and flipped/rotated versions to 342x342 pixels
 - k) Add $Train_img$ and flipped/rotated versions to training set
- 2) Train U-Net with 10,000 iterations selected from the 7200 training images (This corresponds to just over 1 epoch)
- 3) Initialize Threshold as 0.5
- 4) For each of 1800 Training Image:
 - a) Predict the skin lesion area
 - b) Apply Binary Fill Holes
 - c) Use gradient descent to optimize threshold value that maximizes Jaccard Index
- 5) For each test data set image, use optimized threshold to get skin lesion area.
- 6) Apply Binary fill holes

Fig. 4. U-Net Approach with Pre/Post-Processing (Algorithm 1B)

Hair Removal Algorithm

- 1) For each of 2000 images:
 - a) Convert RGB image to greyscale by averaging RGB channels
 - b) Find all hairs in the image using morphological top-hats of disk radius 10
 - c) Use threshold of 0.2 on top-hat output to identify all hair pixels
 - d) Replace hair pixels with median colour of the 30px disc surrounding the pixel of interest.

Fig. 5. Hair Removal Algorithm

Dark Outer Circle Removal Algorithm

- 1) For each of 2000 images:
 - a) Create a circle mask with radius of the length of the image
 - b) while the over 60% of the pixel out of the mask is less than 30:
 - i) Decrement the circle radius by one unit

Fig. 6. Dark outer Circle Removal Algorithms

Clustering Algorithm (Algorithm 2)

- 1) For each of 2000 images:
 - a) Remove hair from image using hair removal technique outlined above
 - b) Rescale image to reduce size
 - c) if image contains dark outer circle:
 - i) Remove outer pixels from area of analysis
 - d) Conduct c-means fuzzy clustering on image pixels within area of analysis $C = 5$
 - e) Group output c-means clusters into 2 groups using K-means clustering
 - f) Output the darker (average of RGB value of cluster centroid) of the two clusters as the area of interest

Fig. 7. Clustering Algorithm

V. RESULTS AND DISCUSSIONS

As discussed in the Methodology section, the segmented images are assessed using the Jaccard Index through 5 random folds validation with 90%-10% train-test split. For the clustering method, since it is completely unsupervised, the average Jaccard Index for the entire data set is also calculated.

The Jaccard index and dice values for 5 different folds are presented in Table 1. Figure 8 shows sample segmentations.

Using U-Nets, for each random fold, the network is trained using the 1800 training images. After training, the average Jaccard Index score is obtained for the remaining 200 test images. This is done for both the U-Net algorithm without pre-/post-processing (Algorithm 1A) and the more complex algorithm with pre-/post-processing (Algorithm 1B).

Examining the Table 1, it is clear that the preprocessing steps (performing histogram equalization, etc.) significantly improved the segmentation results. The average Jaccard Index for Algorithm 1A was 53% with a standard deviation of 2% while the average Jaccard Index for Algorithm 1B was 62% with a standard deviation of 4.7%.

Comparing the U-Net results with state of the art neural networks while it is lower than the top performers at the

2017 ISBI competition, the results were similar to many other submissions using deep networks. For example, the top ISIC 2017 challenge submission, Yuan et al. [10] who used fully convolutional-deconvolutional networks obtained an average Jaccard Index of 0.765. Similarly, Berseth [17] who also used a U-Net obtained the second place in the 2017 challenge with a Jaccard Index of 0.762. There were also many challenge submissions that received a Jaccard Index between 0.444 and 0.665, some of which also used deep neural networks.

The biggest advantage using the proposed algorithm is the number of training iterations required. For example, Yuan et al. trained with 500 epochs on the 2,000 images. Similarly, Berseth trained 200 epochs using 20,000 images (after data augmentation). This means that the two networks above required 1,000,000 and 4,000,000 training iterations, respectively.

In comparison, the networks presented in this paper was trained with only 10,000 training iterations (just over 5 epochs of 1800 images). This means that the network only required 1% of the number of training iterations compared with the other deep network methods. A low number of training iterations is used because the algorithms presented in this paper is designed to work when only low computational power is available (computers without GPUs).

Figure 8 shows a comparison of the skin lesion segmentation algorithms for a few select skin lesion images. The first column in the figure shows the input RGB image. The second column contains the Ground Truth (binary mask manually segmented by a dermatologist). Finally, the third and fourth columns show the output of the U-Net trained with algorithms 1A and 1B respectively. As is evident from the figure, while both

Table 1. Jaccard index (and Dice coefficient in parentheses) for 5 different folds (m is the average and σ the standard deviation).

Fold	Algorithm 1A	Algorithm 1B	Algorithm 2
1	0.54 (0.70)	0.67 (0.80)	0.46 (0.63)
2	0.51 (0.68)	0.61 (0.76)	0.41 (0.58)
3	0.55 (0.71)	0.55 (0.71)	0.44 (0.61)
4	0.54 (0.70)	0.63 (0.77)	0.44 (0.61)
5	0.50 (0.67)	0.65 (0.79)	0.43 (0.60)
m	0.53 (0.69)	0.62 (0.77)	0.44 (0.61)
σ	0.02 (0.02)	0.05 (0.04)	0.02 (0.02)

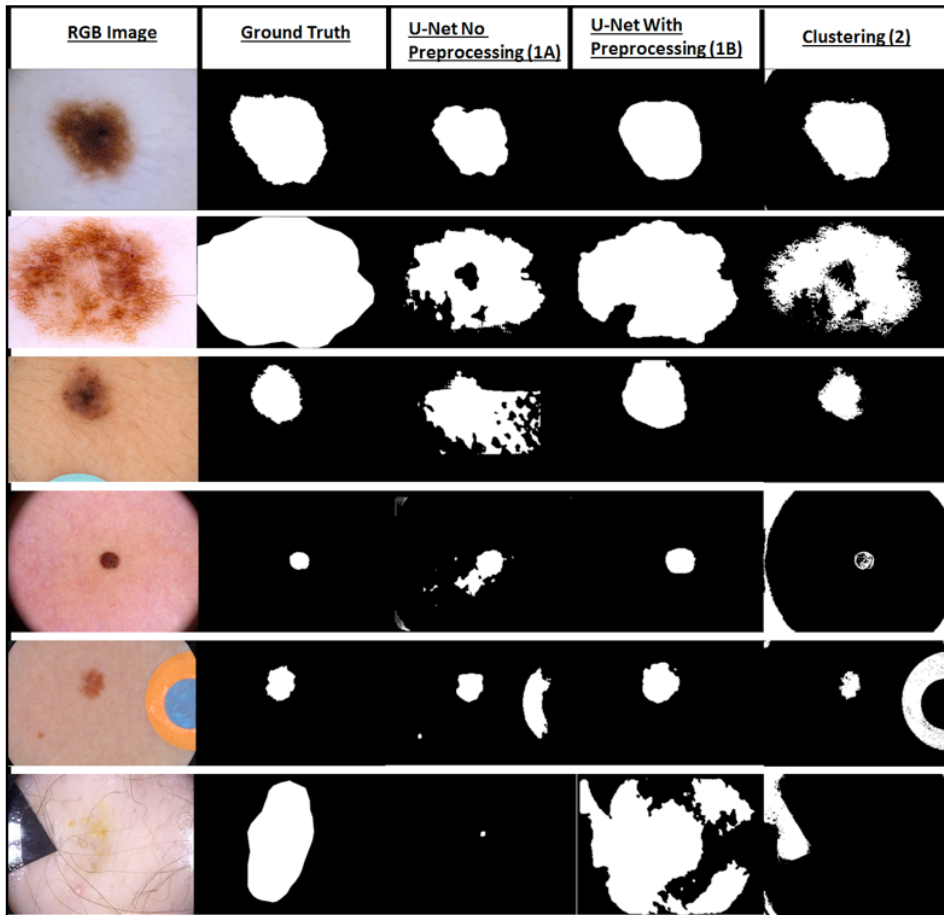


Fig. 8. Sample skin lesion segmentations. Top three rows: Typical examples of most skin lesion images; 3rd and 4rd row: Color variation in skin lesions; 5th row: Medical gauze example.

algorithm 1A and 1B are able to determine the location of the lesion, algorithm 1B is better at determining the border of the skin lesion since algorithm 1A produced a smaller image.

The last three rows show some pathological cases where one or both of the algorithms are unable to properly segment the image. This includes the skin lesion being very small, the presence of another object such as medical gauze or sleeve, and the skin lesion being extremely faint. Looking at the pathological cases, it is clear that the algorithm that performs histogram equalization performs better in most circumstances.

Given that the clustering based approach was unsupervised and did not contain any “training” components, it was not necessary to conduct cross-validation over multiple folds. The output was always going to be the same for every image. However, for the purposes of comparison against the U-nets based approach, the values were calculated for each of the folds used in the earlier results. The Jaccard Index calculated can be found summarized in the Table 1, last column. The Jaccard Index for the entire data set was calculated to be 0.443. This value is quite low in comparison to the values obtained

using U-nets. However, it is important to remember that this algorithm is much simpler and quicker to execute and does not require expensive training.

Figure 8 contains a visualization from the clustering algorithm alongside the output from U-Nets for various image types. Clearly the clustering results are good for images in which no external disturbance exists and color variation is minimized. However, the algorithm performs poorly when artifacts are present. For example, the algorithm incorrectly identifies the black border, the medical gauze, and other dark objects as the skin lesion.

When comparing this with other submissions in the ISIC challenge, this approach would be on par with the 21st place submission. Amongst the competition entries, only one submission followed a clustering based approach submitted by Alvarez et al. [18]. Their solution produced a significantly better result with a Jaccard Index of approximately 0.679. The main reason for this is that their approach uses a much more complex technique to classify the clusters involving an ensemble method which leveraged random forests and support vector machines. When comparing the results from both approaches it is clear by virtue of the Jaccard Index that the U-Net based approach (with preprocessing) is superior.

VI. CONCLUSION AND FUTURE WORK

In conclusion, this paper presented an effective approach to automatically segmenting skin lesions particularly when computers with GPUs may not be available. We described two algorithms, one leveraging U-Nets and another using unsupervised clustering, and put forward effective pre-processing techniques for both approaches to improve the segmentation performance. It is noted that the solutions outlined in this paper are on par with the mid-tier submissions in the ISIC competition while utilizing significantly less training resources than many submissions.

After comparing the clustering and U-Net algorithms, it was clear that U-Nets produce a much better segmentation result, especially using the histogram equalization based pre-processing step. The network only required 1% of the number of training iterations compared with the other deep network methods. This could be particularly beneficial when only low computational power is available (computers without GPUs)

In the future, it would be interesting to find out if the histogram equalization based pre-processing step also significantly improves segmentation performance when the U-Net is trained over hundreds of epochs, instead of just one epoch, with a more powerful GPU similar to the top ISIC 2017 challenge submissions.

REFERENCES

- [1] R. A. Schwartz, *Skin Cancer: Recognition and Management*, 2nd Edition, Massachusetts: Blackwell Publishing Inc., 2008.
- [2] World Health Organization, "Skin Cancers," Ultraviolet radiation and the INTERSUN Programme, 2017. [Online].
- [3] R. Amelard, "High-Level Intuitive Features (HLIFs) for Melanoma Detection," University of Waterloo, Waterloo, 2013.
- [4] D. Gutman, C. C. F. Noel, E. Celebi, B. Helba, M. Marchetti, N. Mishra and A. Halpern, "Skin Lesion Analysis toward Melanoma Detection: A Challenge at the International Symposium on Biomedical Imaging (ISBI)," 2016.
- [5] Melanoma Research Foundation, "The ABCDEs of Melanoma," 2017. [Online]. Available: <https://www.melanoma.org/understand-melanoma/diagnosing-melanoma/detection-screening/abcde-melanoma>. [Accessed 2017 February 2017].
- [6] H. Fan, F. Xie, Y. Li, Z. Jiang and J. Liu, "Automatic Segmentation of Dermoscopy Images using Saliency Combined with Otsu Threshold," *Computers in Biology and Medicine*, vol. in press, 2017.
- [7] M. E. Celebi, G. Schaefer, H. Iyatomi and W. V. Stoecker, "Lesion Border Detection in Dermoscopy Images," *Computerized Medical Imaging and Graphics*, vol. 33, no. 2, pp. 148-153, 2009.
- [8] L. Yu, H. Chen, J. Qin and P.-A. Heng, "Automated Melanoma Recognition in Dermoscopy Images via Very Deep Residual Networks," *IEEE Transactions on Medical Imaging*, vol. 36, no. 4, pp. 994-1004, April 2017.
- [9] R. Garnavi, M. Aldeen, M. E. Celebi, A. Bhuiyan, C. Doliyanitis and G. Varigos, "Automatic Segmentation of Dermoscopy Images Using Histogram Thresholding on Optimal Color Channels," *International Journal of Medicine and Medical Sciences*, vol. 1, no. 2, pp. 126-34, 2010.
- [10] Y. Yuan, M. Chao and Y.-C. Lo, "Automatic Skin Lesion segmentation with fully convolutional-deconvolutional networks," New York, 2017.
- [11] T. Lee, V. Ng, R. Gallagher, A. Coldman and D. McLean, "Dullrazor: A software approach to hair removal from images," *Computers in Biology and Medicine*, vol. 27, no. 6, pp. 533-543, 1997.
- [12] P. Schmid-Saugeon, J. Guillod and J.-P. Thiran, "Towards a computer-aided diagnosis system for pigmented skin lesions," *Computerized Medical Imaging and Graphics*, vol. 27, no. 1, pp. 65-78, 2003.
- [13] R. Melli, G. Costantino and R. Cucchiara, "Comparison of color clustering algorithms for segmentation of dermatological images," *Medical Imaging*, pp. 61443S-61443S, 15 march 2006.
- [14] M. H. Jafari, N. Karimi, E. N. Esfahani, Samavi, Shadrokh, S. M. R. Soroushmehr, K. R. Ward and K. Najarian, "Skin Lesion Segmentation in Clinical Images Using Deep Learning," in *IEEE International Conference on Pattern Recognition (ICPR)*, Cancun, Mexico, 2016.
- [15] J. Akeret, C. Chang, A. Lucchi and A. Refregier, "Radio frequency interference mitigation using deep convolutional neural networks," *Astronomy and Computing*, vol. 18, pp. 35-39, 2017.
- [16] O. Ronneberger, P. Fischer and T. Brox, "U-Net: Convolutional Networks for Biomedical Image Segmentation," in *International Conference on Medical Image Computing and Computer-Assisted Intervention*, Springer International Publishing, 2015.
- [17] M. Berseth, "ISIC 2017 - Skin Lesion Analysis Towards Melanoma Detection," 2017.
- [18] D. Alvarez and M. Iglesias, "k-Means Clustering and Ensemble of Regressions: An Algorithm for the ISIC 2017 Skin Lesion Segmentation Challenge," Oviedo, Spain, 2017.
- [19] Sahba, Farhang, Hamid R. Tizhoosh, and Magdy MMA Salama. "Application of opposition-based reinforcement learning in image segmentation." *Computational Intelligence in Image and Signal Processing*, 2007. CIISP 2007. IEEE Symposium on. IEEE, 2007.
- [20] Shokri, Maryam, and Hamid R. Tizhoosh. "Using reinforcement learning for image thresholding." *Electrical and Computer Engineering*, 2003. IEEE CCECE 2003. Canadian Conference on. Vol. 2. IEEE, 2003.
- [21] Othman, Ahmed, and Hamid Tizhoosh. "Segmentation of breast ultrasound images using neural networks." *Engineering Applications of Neural Networks (2011)*: 260-269.
- [22] Cheng, Kuo-Sheng, Jzau-Sheng Lin, and Chi-Wu Mao. "The application of competitive Hopfield neural network to medical image segmentation." *IEEE transactions on medical imaging* 15.4 (1996): 560-567.
- [23] Ozkan, Mehmet, Benoit M. Dawant, and Robert J. Maciunas. "Neural-network-based segmentation of multi-modal medical images: a comparative and prospective study." *IEEE transactions on Medical Imaging* 12.3 (1993): 534-544.